Journal of Magnetic Resonance **151,** 314–319 (2001)
doi:10.1006/jmre.2001.2383, available online at http://www.idealibrary.com on IDEAL®

Linewidth-Resolved ^{15}N HSQC, a Simple 3D Method to Measure ^{15}N Relaxation Times from T_1 and T_2 Linewidths

Sami Heikkinen* and Ilkka Kilpeläinen†

*Department of Radiology, Helsinki University Central Hospital, P.O. Box 340, FIN-00029, HUCH, Finland; and †Institute of Biotechnology, NMR Laboratory, P.O. Box 56, FIN-00014 University of Helsinki, Finland

Received January 16, 2001; revised May 14, 2001

A three-dimensional approach for measuring ^{15}N relaxation times is described. Instead of selecting particular values for the relaxation period, in the proposed method the relaxation period is incremented periodically in order to create a 3D spectrum. This additional frequency domain of the transformed spectrum contains the relaxation time information in the T_1 and T_2 linewidths, and thus the longitudinal and transverse ^{15}N relaxation times can be measured without determination of 2D cross peak volumes/intensities and subsequent curve fitting procedures.

Key Words: **relaxation; protein; 3D experiment; linewidth; ubiquitin; ^{15}N HSQC.**

INTRODUCTION

Continuous interest has been focused on measuring relaxation times, T_1, T_2, and $T_{1\rho}$. These time constants provide information over the dynamic behavior of the molecule in question. In protein NMR, characterization of ^{15}N and ^{13}C relaxation times (T_1, T_2, and $T_{1\rho}$) and heteronuclear NOE-values are commonly used in studying global protein motions as well as internal backbone mobility (*1–6*). Further, the use of ^{15}N relaxation times in combination with residual dipolar coupling information ($^1D_{NH}$) allows the identification of conformational exchange of protein backbone, as there is a structure dependence of ^{15}N T_1/T_2 ratios and dipolar couplings in anisotropically tumbling proteins (*7*).

Although a wealth of relaxation data for protein could be collected if T_1, T_2, and $T_{1\rho}$ were measured for ^{1}H, ^{13}C, and ^{15}N, it is quite common routine to limit the relaxation measurements to ^{15}N, as this data combined with ^{15}N{^{1}H}-NOE measurements usually provide enough information to determine the dynamic properties of a protein backbone. The ^{15}N T_1, T_2, and $T_{1\rho}$ values are usually measured by recording a set of 2D ^{15}N-HSQC spectra with different delays (T_r) during which the relaxation (longitudinal or transverse) causes decay of signal intensity. The volumes (or intensities) of cross peaks are then measured as a function of delay T_r, and subsequent fitting of volumes (or intensities) to exponential function results in the relaxation time values (*1–4*). The main inconvenience of this method is the integration of the 2D cross peak volumes, a task that is quite prone to errors. The volume integrations can be circumvented by employing the constant-time accordion experiment (*8–11*). In this method, the relaxation period T_r is covaried in concert with the t_1 period, and thus the relaxation time domain, T_r, is projected onto t_1 domain (*10, 11*). This accordion relaxation data is analyzed in the t_1 domain using HSVD (*12*) and Levenberg–Marquardt algorithms (*13*) in order to obtain relaxation times.

We have tried to find a method enabling the collection of reliable relaxation data avoiding the necessity to (a) determine volumes or intensities of 2D cross peaks and (b) perform separate curve fitting procedure. An experiment that fullfills these conditions can be readily constructed by discarding the constant time evolution, as well as the accordion approach from pulse sequences described by Mandel *et al.* (*10*) and Carr *et al.* (*11*), but returning to the true 3D experiment instead, where the relaxation period T_r is independently incremented. Thus, the relaxation information is directly coded into the lineshape in the particular frequency domain. Now, in the resulting 3D spectrum two of the frequency domains form a convetional 2D ^{15}N HSQC spectrum, and the third domain contains the lineshape. Although the current approach is a direct application of ideas presented previously, to the best of our knowledge this kind of 3D experiment has not been described in order to determine ^{15}N relaxation times for proteins. It allows a simple and robust measurement of relaxation times from "relaxation" linewidths, and can be easily adopted for other heteronuclei as well.

DESCRIPTION OF THE METHOD

The 3D pulse sequences for the measurement of ^{15}N T_1 and T_2 are shown in Figs. 1A and 1B, respectively. The presented pulse sequences are essentially similar to the 2D versions presented by Kay *et al.* with suppression of the interference from the dipolar/CSA cross-correlation contribution (*14*). There are only a few differences including the incrementation of the T_r period to create the third frequency dimension, an additional string of ^{15}N 180° pulses in T_2 measurement, and purge periods prior to incremented T_r domain in both sequences. These differences will be discussed later in the text. For larger proteins, the pulse sequences presented in Fig. 1 can be modified for

1090-7807/01 $35.00

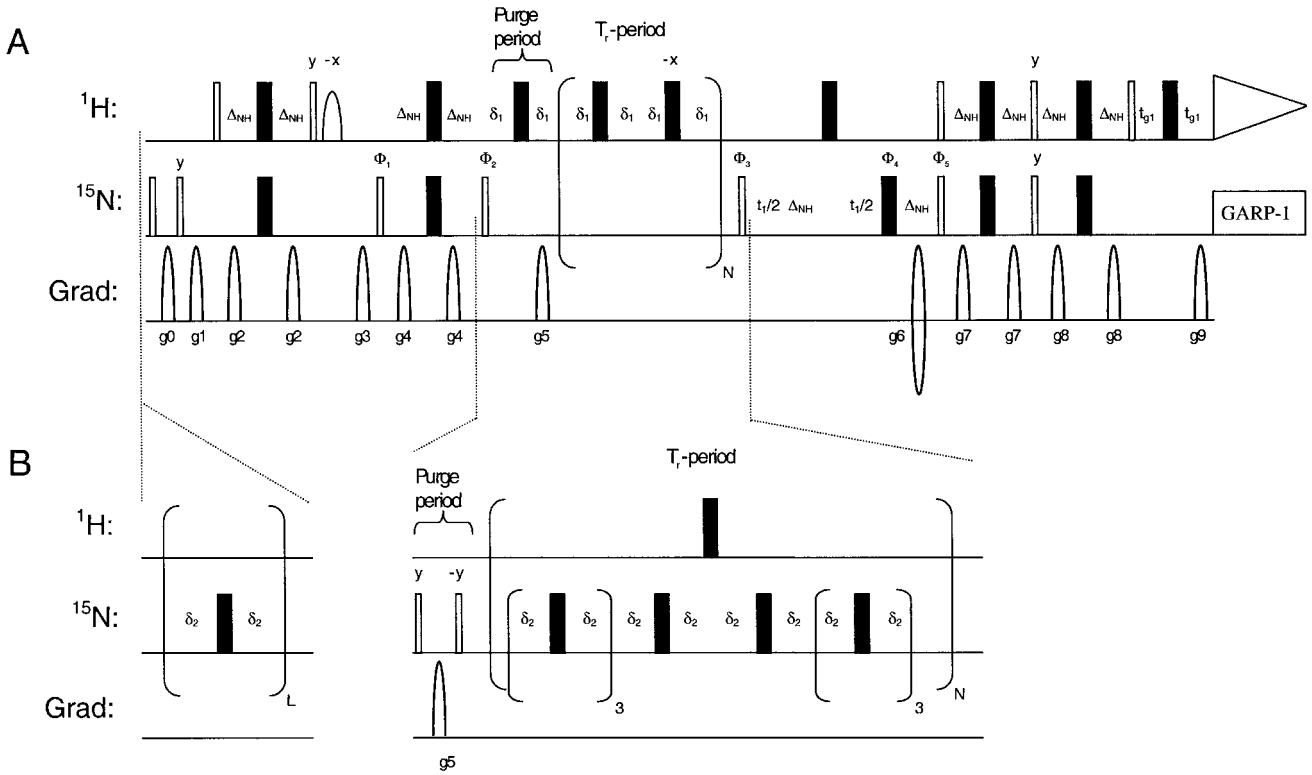

FIG. 1. The 3D experiments for the measurement of ^{15}N relaxation times T_1 and T_2. Pulse sequence for (A) T_1 measurement and (B) T_2 measurement. Narrow (wide) bars correspond to 90° (180°) hard rectangular pulses. Gradient pulses are represented by narrow white half-ellipses denoted by g0–g9. White half-ellipse on ^{1}H-channel represents a selective 90° sinc-pulse on water resonance. The ^{1}H and ^{15}N-carrier positions are 4.7 (water) and 113.0 (center of ^{15}N-spectral region). All the pulses have x phase unless otherwise indicated. Delays: $\Delta_{NH} = 1/4^1J_{NH}$, t_1 = incremented delay (^{15}N shift evolution), t_{g1} = gradient duration plus recovery delay, δ_1 and δ_2 = basic delays which define the duration of T_r element (typically δ_1 = 2.5–5.0 ms and δ_2 = 0.450–0.650 ms). Decoupling of ^{15}N during the acquisition was accomplished using the GARP-1 sequence (*20*). Incrementation of T_r period is achieved by incrementing the loop counter N by suitable integer $N_{(inc)}$. For T_2 measurement, the loop counter L is decremented from maximum value to 0 in course of T_r incrementation. The aforementioned element ensures that the number of applied ^{15}N 180° pulses and thus the induced heat is constant throughout the experiment. The phase cycle employed for sequence A is $\Phi_1 = x, -x$, $\Phi_2 = 16(y), 16(-y)$, $\Phi_3 = 2(-y), 2(y)$, $\Phi_4 = 4(x), 4(y), 4(-x), 4(-y)$, $\Phi_5 = x$, receiver $= x, 2(-x), x, -x, 2(x), -x, x, 2(-x), x, -x, 2(x), -x, -x, 2(x), -x, x, 2(-x), x, -x, 2(x), -x, x, 2(-x), x$. The phase cycle for sequence B is $\Phi_1 = x, -x$, $\Phi_4 = 2(x), 2(y), 2(-x), 2(-y)$, $\Phi_5 = x$, receiver $= x, 2(-x), x$. In both experiments, the N- and P-type coherences are recorded separately by inverting the sign of gradient g6 and the phase Φ_5 in synchrony. Axial peak displacement was obtained via the States-TPPI method (*21*) by inverting the phase Φ_1 and receiver on every second increment.

better signal-to-noise ratio by simply replacing the sensitivity enhanced HSQC (*15*) with the TROSY sequence (*16–19*).

As neither chemical shift nor coupling evolution are active during the T_r period, the resulting time dependence of the magnetization can be presented by

$$I(T_r) = I_0 \exp(-T_r / T_{1,2}), \qquad [1]$$

where $T_{1,2}$ is either longitudinal or transverse relaxation time, depending on the pulse sequence used.

After Fourier transformation, this exponentially decaying signal in the T_r time domain results in Lorentzian lineshape in the frequency domain, with the linewidth (FWHH) determined by Eq. [2], and thus relaxation time can be coveniently determined:

$$\mathrm{FWHH} = 1/(\pi T_{1,2}). \qquad [2]$$

The actual incrementation of the T_r period is accomplished by incrementing the loop counter N (Fig. 1), i.e., the number of repetitions of the basic T_r element, by a suitable number (integer). For example, we selected a spectral width of 10 Hz for the third frequency dimension (SW_{LW}) in the T_1 measurement of ubiquitin (Fig. 2). Because the delay δ_1 was set to 2.5 ms, the time increment of 100.0 ms corresponding the SW_{LW} can be achieved by incrementing the loop counter N by $N_{(inc)} = 10$. Since the basic T_r-element has finite length, the "available" spectral widths are limited to some degree, although there is the possibility of making small adjustments to the length of the basic T_r element by changing the interpulse delays δ_1 and δ_2 (*14*). The total length of the basic T_r element for the T_1 measurement is $4\delta_1$ and $8\delta_2$ for the T_2 measurement; i.e., ^{1}H and ^{15}N 180° pulses are fitted in delays δ_1 and δ_2. As the relaxation time is directly extracted from the linewidth, the use of window functions prior to zero-filling and Fourier transform is prohibited. Due to this fact, T_r(max) must be

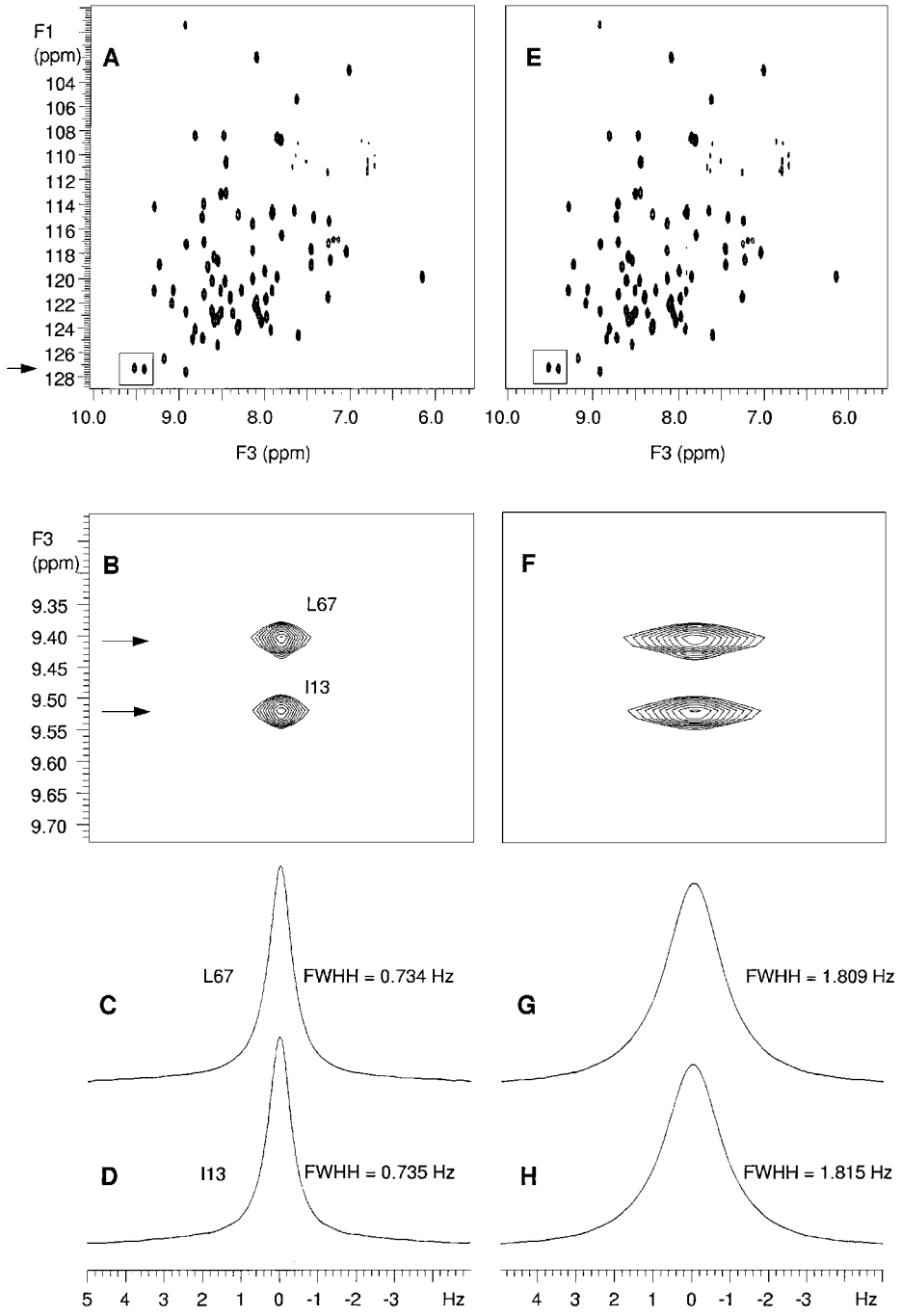

FIG. 2. 2D planes and 1D traces of 3D T_1 (Figs. A–D) and T_2 experiments (Figs. E–H) acquired from 1.0 mM uniformly ^{15}N-labeled ubiquitin, 90/10% H_2O/D_2O, 30°C at 600 MHz. The 3D spectra were recorded using pulse sequences presented in Fig. 1: (A, E) 2D HSQC plane; (B, F) expansions of 2D planes for taken at ^{15}N-shift position marked by an arrow in A; (C, D, G, H) 1D traces taken along linewidth-axis in Figs. B and F (horizontal axis), position from where the traces are taken are marked with arrows. Traces C, G, D, and H are taken at the positions indicated by upper and lower arrow, respectively. The measured linewidth is marked in Figs. C, D, G, and H. The 3D T_1 and T_2 experiments were performed using a Varian Unity INOVA 600 spectrometer. Spectral widths were 8000 Hz (^{1}H) and 2000 Hz (^{15}N) for both experiments. T_1 experiment and T_2 experiment were acquired using spectral width of 10 Hz ($N_{(inc)} = 10$) and 25 Hz ($N_{(inc)} = 4$) for linewidth-domain (SW_{LW}), respectively. The initial value for the loop counter L of the T_2 experiment was 224. The ^{1}H and ^{15}N carrier positions were 4.7 (water) and 113.0 ppm (center of the ^{15}N spectral region. The T_1 experiment was acquired using 8 transients, 2048 (^{1}H, complex points) × 100 (^{15}N, complex points) × 18 (linewidth-domain, real points). The same number of transients and increments were used in the T_2 experiment except only 8 increments (real points) in linewidth-domain were performed. A combination of squared cosine bell and gaussian apodization function was applied in ^{1}H and ^{15}N dimensions. Linear prediction was applied in both experiments to extend linewidth-domain by 18 and 16 real points in the T_1 and T_2 experiments, respectively. Matrices were zero filled to 2048 (^{1}H) × 256 (^{15}N) × 512 (linewidth-domain, real points) prior to Fourier transform. Pulses: ^{1}H 90° = 5.1 μs; ^{15}N 90° = 9.5 μs; water selective 90° pulse = 1.422 ms (one-lobe sinc at RF power of 175 Hz). Delays: relaxation delay = 2.5 s, $\Delta_{NH} = 2.63$ ms, $t_{g1} = 0.350$ ms, $\delta_1 = 2.5$ ms, and $\delta_2 = 0.625$ ms. Gradient strengths (durations): g0 = 16.0 G/cm (0.5 ms), g1 = 11.2 G/cm (0.5 ms) g2 = 16.0 G/cm (0.5 ms), g3 = 22.0 G/cm (1.0 ms), g4 = 16.0 G/cm (1.0 ms), g5 = 36.0 G/cm (1.25 ms), g6 = 26.0 G/cm (2.5 ms), g7 = 4.0 G/cm (0.5 ms), g8 = 6.0 G/cm (0.5 ms), g9 = 26.0 G/cm (0.25 ms). All the gradients were block shaped. ^{15}N-decoupling during the acquisition was achieved using GARP-1 (20).

relatively long in order to ensure sufficient decay of magnetization and thus the suppression of truncation artifacts. Fortunately, as the needed spectral width in the linewidth domain (SW_{LW}) is usually small (and correspondinly the time increment is long), long enough T_r(max) can be reached with relatively few time increments. Furthermore, as only the decay of the signal intensity takes place during the T_r period, the data is purely real and thus one spectrum per $1/SW_{LW}$ increment is sufficient. Additional reduction of the experimental time can be easily achieved by using linear prediction to calculate signal decay in the T_r domain. This possibility is of particular importance when T_2 values are to be measured. In T_2 measurement using the linewidth method, relatively long T_r(max) of about 500–750 ms would be needed to ensure sufficient decay of magnetization in order to avoid truncation artifacts. Long T_r periods (during which the modified CPMG pulse train is applied) may cause undue sample heating and may also eventually damage the probe. Therefore, in addition to obtained reduction of experimental time, it could be beneficial to use short T_r(max) and utilize linear prediction to extend the signal in the T_r domain. As mentioned above, compared to the sequence for T_2 measurement described by Kay *et al.*, the pulse sequence presented in Fig. 1B contains an additional string of ^{15}N 180° pulses (loop counter L). This element is incorporated in the sequence in order to minimize the possible effects of sample heating in the course of T_r incrementation (increasing number of ^{15}N 180° pulses). The loop counter L starts from maximum value of $8 * N_{(inc)} * (ni(T_r) - 1)$, where $ni(T_r)$ is the number of increments in T_r domain and is decremented by $8 * N_{(inc)}$, whenever loop counter N is incremented. Another difference from the original pulse sequence is gradient purging period, $90^\circ_y(^{15}N)$-*gradient*-$90^\circ_{-y}(^{15}N)$, prior to the modified CPMG pulse-train. The purpose of this purging period is to destroy all ^{15}N magnetization that is not refocused during the preceding Δ_{NH}-$180^\circ(^1H)$, $180^\circ(^{15}N)$-Δ_{NH}-period. Gradient purging is performed prior to the actual T_r element, as presented in Fig. 1A. All the ^{15}N magnetization that is not aligned along the *z* axis is destroyed by the gradient applied during the first δ_1 delay in propagator $90^\circ_{\phi 2}(^{15}N)$-$\delta_1$-$180^\circ(^1H)$-$\delta_1$.

RESULTS AND DISCUSSION

The measurement of relaxation times T_1 and T_2 with 3D pulse sequences presented in Fig. 1 was demonstrated using 1 mM uniformly ^{15}N labeled ubiquitin (VLI Research) dissolved in 90/10% H_2O/D_2O, pH 4.7, 50 mM sodium phosphate buffer, at 30°C. All the experiments were carried out using Varian Unity Inova 600 spectrometer equipped with a $^1H/^{13}C/^{15}N$ triple resonance, actively shielded *z*-gradient probe. The relaxation times for selected 30 residues were extracted from linewidths in the dedicated frequency domain using Eq. [2]. The linewidths can be measured either manually (a method that is not completely objective), or by using a robust linewidth-determination method, which looks for maximum peak-top intensity and subsequently determines two data points representing the linewidth. In this work, we utilized the standard Varian Vnmr6.1d software macro for linewidth measurement (dres-command). Figure 2 presents the determination of T_1 and T_2 relaxation times for residues I13 and L67 using 2D expansions and 1D traces taken from the 3D spectra. Figures 2A–2D and 2E–2H correspond to 3D T_1 and T_2 experiments, respectively. Figures 2A and 2E show the 2D ^{15}N HSQC planes of the 3D spectra. The cross peaks of residues I13 and L67 are located in the area marked with a box. Figures 2B and 2F show expansions of 2D planes of the 3D spectra taken at the positon in the ^{15}N axis marked with arrow. The cross peaks shown in these 2D planes contain the relaxation information coded into the linewidths. In order to measure the linewidths, the 1D traces were selected (traces are taken at the positions marked with arrows in Fig. 2B and corresponding 1D traces are shown in Figs. 2C, 2D, 2G, and 2H). In order to achieve as reliable relaxation times as possible, the 1D trace should be selected from the midpoint of the 2D contour (i.e., by selecting the maximum intensity 1D trace), although in theory, the linewidth in one dimension should be the same throughout the contour. In practice, deviations occur and are likely due to the S/N-ratio-drop induced errors in linewidth measurement when off-center 1D-traces are selected. In our case, the 1D traces were taken from the plane where the other axis was ^{1}H (resolution 7.8 Hz/pt). The extraction of the 1D trace one point off from the center of the contour (maximum intensity 1D trace) resulted in an average error of about 4% in T_1 values (10 residues were checked). The corresponding average error for the T_2 values was 1%. Smaller errors in T_2 values can be explained by the fact that the same amount of deviation in the linewidth measurement alters the T_2 result less, as the linewidth corresponding to T_2 is significantly larger. If better numerical resolution on the ^{1}H axis was utilized, it could be assumed then that the misselection of 1D trace by one point in ^{1}H-domain had a smaller effect on the results. In the case of peak-top overlap, one naturally must select a 1D trace from the region far from the overlapping contour center. In such cases, good numerical resolution could be useful in order to have continuous lineshape in the ^{1}H-dimension (or ^{15}N, depending on which 2D plane is used to determine the linewidths). Good resolution of the other chemical shift axis (in our case ^{15}N), in turn, would improve the accuracy of the 2D-plane selection. One factor, which also may affect the results, is phasing. Therefore, careful phase adjustments in all dimensions are recommended. The extracted 1D-traces were corrected for DC-offset. This ensured that macro (dres-command) used to measure linewidths performed correctly. It should be noted that extremely fine resolution in this linewidth-domain is crucial as relatively narrow linewidths must be measured accurately. The measured linewidths were converted into relaxation time data by using Eq. [2]. To compare the results obtained using the current approach, standard relaxation time analyses were performed for 3D data sets; i.e., the 2D ^{15}N HSQC planes (corresponding to particular T_r value) were Fourier transformed and cross-peak volumes were measured as a function of T_r. The volume integration was performed using standard Vnmr6.1B software.

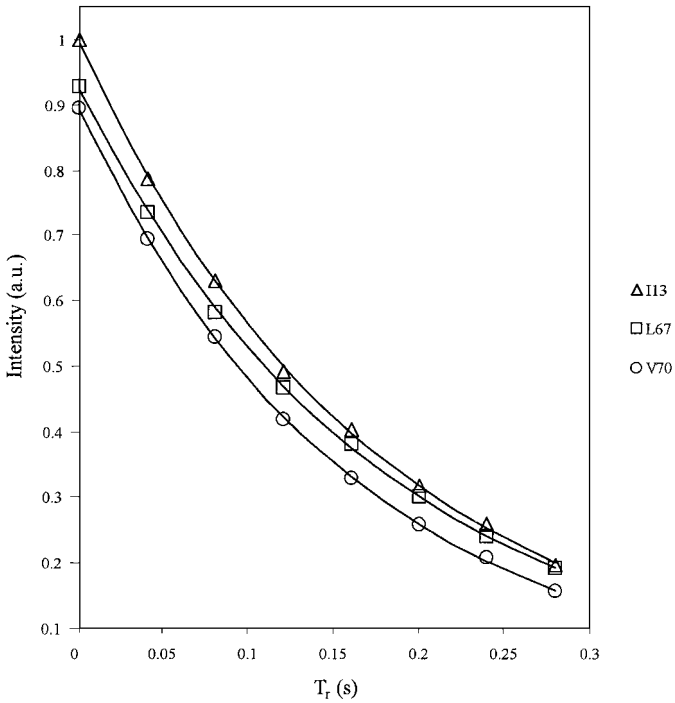

FIG. 3. Experimental ^{15}N T_2 data of three residues I13, L67, and V70. The solid curves represent the best least square fits of the exponential function while the experimentally determined volumes are indicated with triangle, square, and circle for residues I13, L67, and V70, respectively. The presented experimental data is extracted from the 3D experiment as described in the text. The first experimental data point is recorded with T_r-value 0.0 ms and subsequent points with steps of 40.0 ms, which corresponds to the selected $SW_{LW} = 25$ Hz for the 3D T_2 experiment. The last data point was recorded with $T_r = 280.0$ ms.

Subsequent linear least-squares fitting of volumes to the exponential function (Eq. [1]) was used to extract the relaxation times. Figure 3 presents volumes of 2D cross peaks from T_2 measurement as a funtion of delay T_r and corresponding fitted exponential functions for three residues, I13, L67, and V70. Table 1 collects the T_1 and T_2 values measured with standard and linewidth techniques, and a corresponding graphical presentation is shown in Fig. 4. This plot, as well as Table 1, confirm that reliable values for relaxation times T_1 and T_2 can be obtained from linewidths using the proposed 3D pulse sequences. There are some visible differences between the two methods, but by percentage these are relatively small. These differences might be due to the somewhat limited numerical resolution in the linewidth domain (which causes an average uncertainty of 2.8% in linewidth determination for both T_1 and T_2 experiments). In addition to increasing the digital resolution, also fitting of Lorenzian lines could improve the accuracy of the current 3D methods. Particularly biased results are obtained for residue G76, which has relatively long T_1 and T_2 values compared to the relaxation times observed for other residues. Due to long relaxation times of G76, there is a significant amount of intensity left in the data point corresponding to T_r(max). Subsequent linear prediction (onefold for T_1 measurement and twofold for T_2 measurement for the presented relaxation data) was not sufficient to decay the signal intensity enough to avoid truncation artifacts in the linewidth domain. For other residues, no truncation artifacts were observed, and a good agreement of relaxation time results between classic and linewidth-based methods was obtained. Therefore, the current linewidth-based method must be interpreted with caution whenever severe truncation wiggles in the linewidth domain are observed. Fortunately, such residues can still provide reliable relaxation time information as the 3D data also permits the use of the classic volume/intesity measurement approach.

In order to perform a successful 3D linewidth-resolved experiment, a crude estimation of average relaxation times (T_1 or T_2) is needed. This enables the user to select sufficient spectral width, SW_{LW}, and the number of increments for the linewidth-domain to ensure the needed decay of the signal in the course of T_r incrementation. Notably, the average T_1 and T_2 values can be readily estimated from the decay of amide proton signals

TABLE 1

Comparison of ^{15}N T_1 and T_2 Values for 30 Residues of ^{15}N-Labeled Ubiquitin Obtained Using Classic Curve-Fitting Procedures, T_1(Fit) and T_2(Fit), and 3D Linewidth Approach, T_1(3D) and T_2(3D)

Residue	T_1(Fit) [s]	T_1(3D) [s]	T_2(Fit) [s]	T_2(3D) [s]
Q2	0.449	0.451	0.176	0.172
I3	0.435	0.444	0.181	0.164
F4	0.422	0.416	0.177	0.179
V5	0.444	0.450	0.186	0.188
K6	0.433	0.436	0.174	0.178
T7	0.432	0.434	0.176	0.174
L8	0.392	0.418	0.189	0.178
I13	0.438	0.433	0.174	0.177
L15	0.436	0.438	0.172	0.174
V17	0.428	0.429	0.176	0.173
E18	0.456	0.471	0.178	0.179
K27	0.420	0.403	0.172	0.168
I30	0.434	0.417	0.185	0.178
D32	0.439	0.420	0.186	0.181
E34	0.458	0.442	0.187	0.182
Q40	0.439	0.428	0.179	0.179
L43	0.441	0.442	0.178	0.174
I44	0.435	0.443	0.173	0.182
F45	0.435	0.436	0.159	0.165
L50	0.442	0.429	0.165	0.174
D52	0.491	0.481	0.187	0.178
L56	0.411	0.399	0.177	0.168
N60	0.438	0.419	0.181	0.173
E64	0.427	0.426	0.176	0.175
S65	0.425	0.420	0.173	0.171
T66	0.429	0.430	0.183	0.180
L67	0.435	0.434	0.177	0.176
H68	0.442	0.439	0.183	0.185
V70	0.430	0.415	0.161	0.163
G76	1.220	1.159	0.797	0.389

Note. Experimental parameters are described in the legend of Fig. 2.

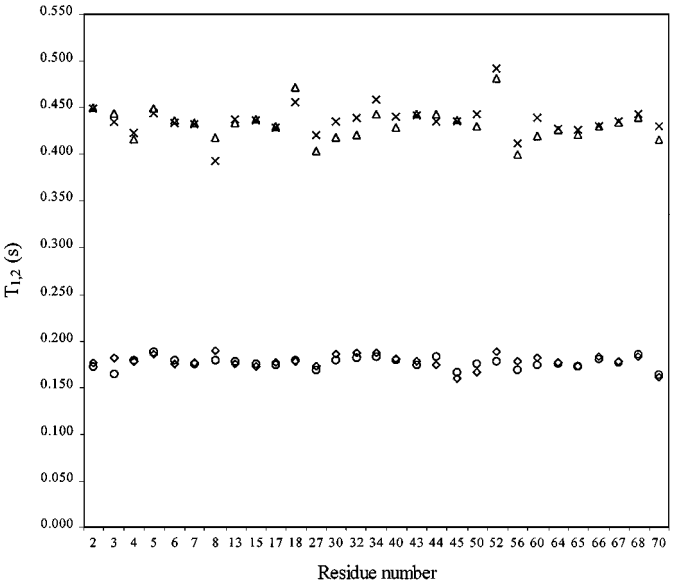

FIG. 4. Graphical plot of data shown in Table 1. Relaxation times (^{15}N T_1 and T_2) of residue G76 are omitted from the plot. Longitudinal ^{15}N relaxation times obtained using standard curve fitting and linewidth techniques are represented by cross and triangle, respectively, whereas the transverse ^{15}N relaxation times are represented by diamonds (fit) and circles (linewidth).

from a 1D relaxation series. In practice, selecting the number of increments so that T_r(max) is at least 1.0–2.0 times the average relaxation time, reliable relaxation data for most residues can be collected after performing one- or twofold extension of time domain using linear prediction. Of course, if the spectrometer time is not restricted, one can always use more increments in the linewidth-domain, especially for the T_1-measurement. For the T_2-measurement, this is also possible if sample cooling-air of the spectrometer's temperature regulation unit can maintain the desired temperature and if the probe can tolerate a long string of ^{15}N 180° pulses. In our hands, the T_2 results obtained using the linewidth method after data extension via twofold linear prediction were essentially similar to those obtained with standard T_2 measurement techniques, suggesting that one can use linear prediction procedures to extend data with predicted points at least twice the number of the original points.

In conclusion, the current 3D linewidth-based experiments allow the measurement of ^{15}N T_1 and T_2 relaxation times very conveniently from linewidths without separate volume/intensity measurement and fitting procedures. This should also hold for $T_{1\rho}$ measurements, as such an experiment can be readily constructed by modifying the pulse sequence presented in Fig. 1B. The time needed to perform these 3D experiments described is not much longer than performing a series of 2D experiments with selected T_r values. This arises from the fact mentioned earlier in the text that the data in the T_r domain is real and thus no imaginary part must be collected. In addition, further shortening of the needed experimental time can be readily achieved by extending the T_r domain with the aid of linear prediction. Furthermore, since the linewidths are used instead of 2D cross-peak volumes/intensities to determine ^{15}N relaxation times, a good signal-to-noise ratio is not as crucial, as in the classic approach.

ACKNOWLEDGMENT

This work was supported by the Academy of Finland.

REFERENCES

1. J. W. Peng and G. Wagner, *Methods Enzymol.* **239,** 563–596 (1994).
2. L. E. Kay, D. A. Torchia, and A. Bax, *Biochemistry* **28,** 8972–8979 (1989).
3. G. M. Clore, P. C. Driscoll, P. T. Wingfield, and A. M. Gronenborn, *Biochemistry* **29,** 7387–7401 (1990).
4. J. W. Peng and G. Wagner, *J. Magn. Reson.* **98,** 308–332 (1992).
5. P. Luginbühl, K. V. Pervushin, H. Iwai, and K. Wüthrich, *Biochemistry* **36,** 7305–7312 (1997).
6. S. F. Lienin, T. Bremi, B. Brutscher, R. Brüschweiler, and R. R. Ernst, *J. Am. Chem. Soc.* **120,** 9870–9879 (1998).
7. E. de Alba and N. Tjandra, *J. Magn. Reson.* **144,** 367–371 (2000).
8. G. Bodenhausen and R. R. Ernst, *J. Magn. Reson.* **45,** 367–373 (1981).
9. L. E. Kay and J. H. Prestegard, *J. Magn. Reson.* **77,** 599–605 (1988).
10. A. M. Mandel and A. G. Palmer III, *J. Magn. Reson. A* **110,** 62–72 (1994).
11. P. A. Carr, D. A. Fearing, and A. G. Palmer III, *J. Magn. Reson.* **132,** 25–33 (1998).
12. H. Barkhuijsen, R. de Beer, and D. van Ormondt, *J. Magn. Reson.* **73,** 553–557 (1987).
13. W. H. Press, B. P. Flannery, S. A. Teukolsky, and W. T. Vetterling, "Numerical Recipes: The Art of Scientific Computing," 2nd ed., Cambridge Univ. Press, Cambridge, UK (1986).
14. L. E. Kay, L. K. Nicholson, F. Delaglio, A. Bax, and D. A. Torchia, *J. Magn. Reson.* **97,** 359–375 (1992).
15. L. E. Kay, P. Keifer, and T. Saarinen, *J. Am. Chem. Soc.* **114,** 10,663–10,665 (1992).
16. K. Pervushin, R. Riek, G. Wider, and K. Wüthrich, *Proc. Natl. Acad. Sci. U.S.A.* **94,** 12,366–12,371 (1997).
17. J. Weigelt, *J. Am. Chem. Soc.* **120,** 10,778–10,779 (1998).
18. M. H. Lerche, A. Meissner, F. M. Poulsen, and O. W. Sørensen, *J. Magn. Reson.* **140,** 259–263 (1999).
19. T. Schulte-Herbrüggen and O. W. Sørensen, *J. Magn. Reson.* **144,** 123–128 (2000).
20. A. J. Shaka, P. B. Barker, and R. Freeman, *J. Magn. Reson.* **64,** 547–552 (1985).
21. D. Marion, M. Ikura, R. Tschudin, and A. Bax, *J. Magn. Reson.* **85,** 393–399 (1989).